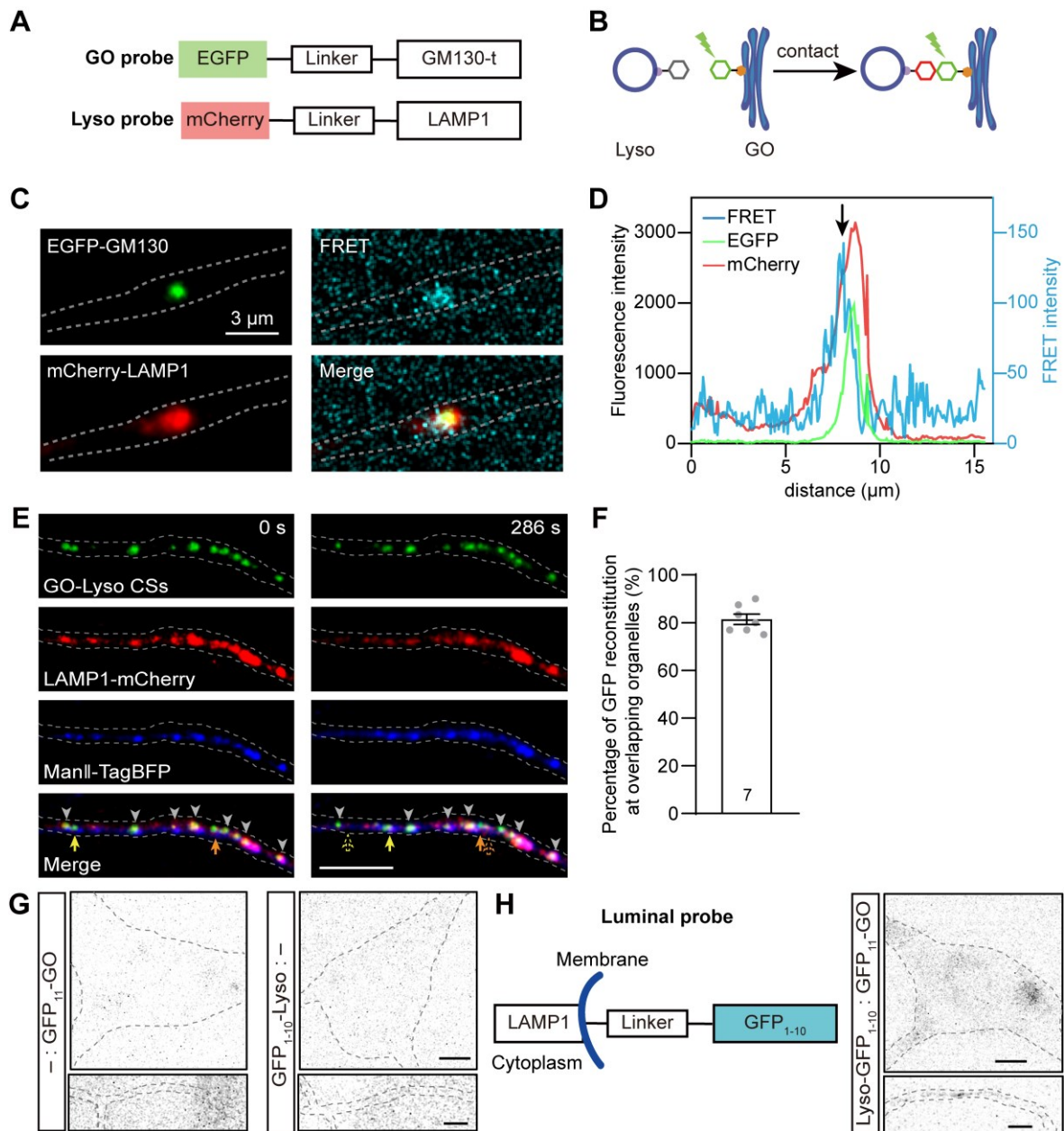


1 **Supplementary information, Figure S1**



2

3 Figure S1 Check the accuracy of the split-GFP probes using for labeling CSs in dendrites. (A-D) The

4 detection of GO-Lyso CSs with the alternative FRET probes. (A) Schematic diagram of the GO and

5 Lyso FRET probes. (B) Cartoon showing the detection of GO-Lyso CSs using the FRET probes. (C)

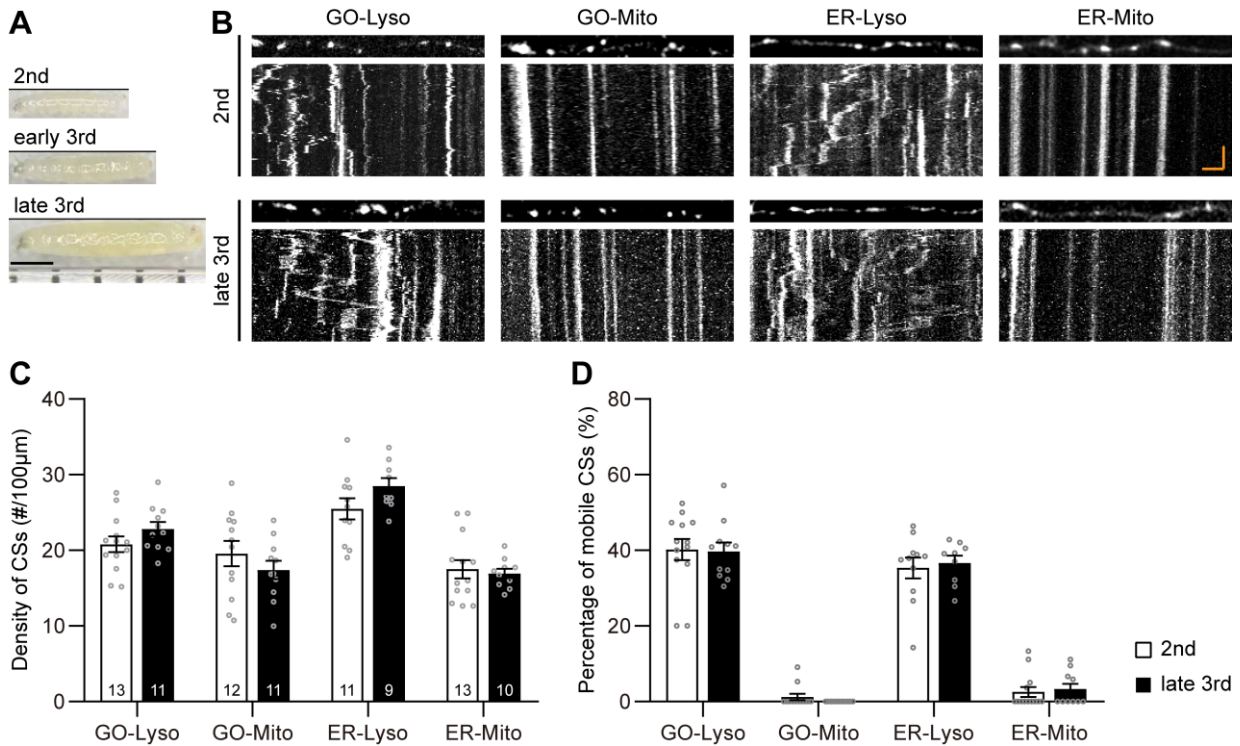
6 Confocal images showing the FRET signal (cyan) colocalized with GO (green) and Lyso (red) in

7 dendrite expressing the complementary GO and Lyso FRET probes. (D) Fluorescence intensities of

8 the three channels in the dendritic region in (c). Arrow indicates the site of FRET signal. (E, F)

9 Check the position of the reconstructed GFP. (E) Three-color time-lapse images showing the co-  
10 localization and co-movement of split-GFP probes labelled CSs with two organelles (GOs: ManII-  
11 mTagBFP2, Lyso: Lamp1-mCherry). Arrowheads indicate the co-localized contact sites with  
12 organelles; the yellow arrows indicate co-movement. (F) Quantitative analysis of the proportion of  
13 GFP reconstitution at two overlapped organelles labelled with fluorescent proteins. The number in  
14 the bar diagram represents the sample size from three *Drosophila* larvae. Data are the means  $\pm$  SEM.  
15 (G) Representative images showing that no apparent GFP signal was detected when GFP<sub>11</sub> or GFP<sub>1-10</sub>  
16 were expressed alone. (H) Leaking test of split-GFP probes through co-expressing the luminal  
17 lysosomal probe (left) and GO probe in C3da neurons showing no reconstituted GFP puncta were  
18 detected (right). Scale bar: 3  $\mu$ m in (C), 2  $\mu$ m in soma and 10  $\mu$ m in dendrites in (E), (G) and (H).  
19

20 **Supplementary information, Figure S2**



21

22 Fig. S2 Organization patterns of the four CSs in dendrites during larva development. (A)

23 Photographs of larvae at different ages. (B) Representative confocal images and the corresponding

24 kymographs showing the distribution and movement of four types of the GELM CSs in second

25 (upper) and late third (bottom) instar larvae. (C and D) Quantitative analysis of the CS density (C)

26 and motility (D) in larvae at different ages. The numbers in the bar diagram represent the sample

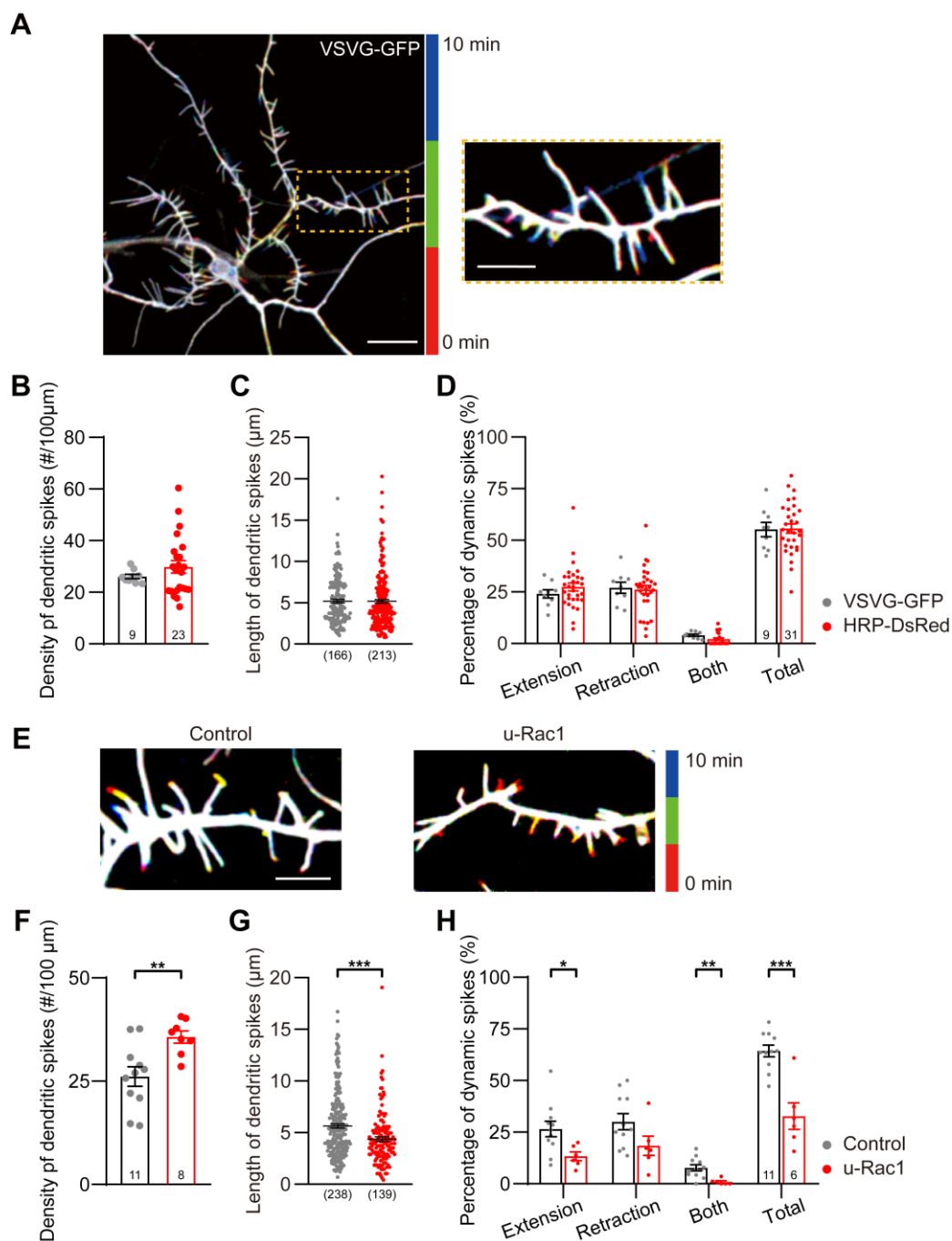
27 sizes of each experimental group from three to six *Drosophila* larvae. For all quantifications, data are

28 the means  $\pm$  SEM. Unpaired Student's t-test in (C and D) showing no significant difference. Scale

29 bars: 1 mm in (A); horizontal scale bar: 4  $\mu$ m and vertical bar: 2 min in (B)

30

31 **Supplementary information, Figure S3**



32

33 Figure S3 The ectopic expression of Rac1 alters the structural plasticity of dendritic spikes. (A)

34 Temporal-code images from time-lapse imaging of dendritic spikes labeled with VSVG-GFP for 10

35 min. The area of the dotted box in (left) is enlarged in (right). Scale bars in left: 20  $\mu$ m, right: 10  $\mu$ m.

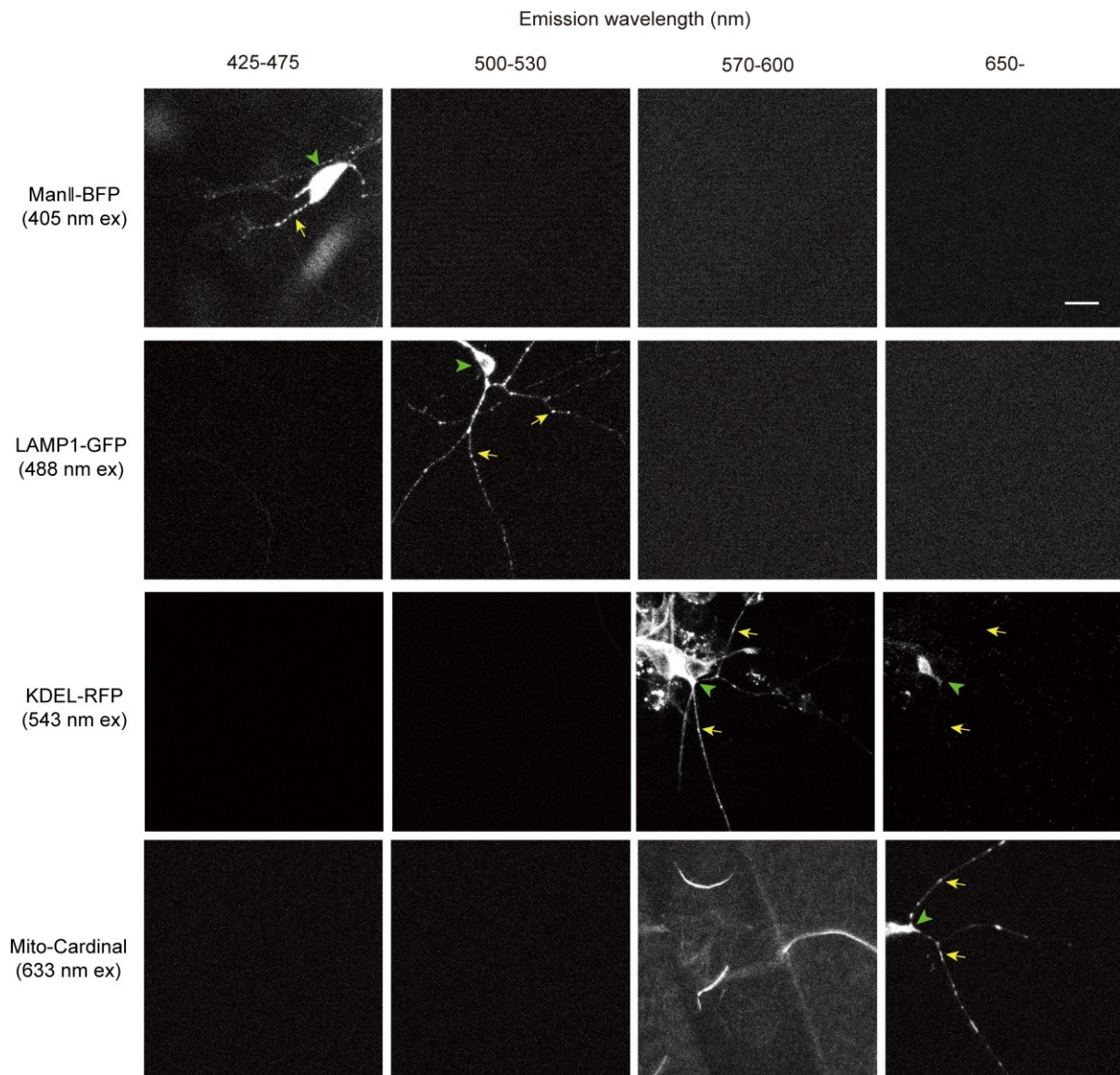
36 (B-D) Comparison of the structural plasticity of dendritic spikes labeled with VSVG-GFP to that

37 labeled with HRP-DsRed. Density in (B), length in (C) and dynamics in (D). (E) Temporal-code

38 images from time-lapse imaging showing the dynamic dendritic spikes under the normal condition  
39 and the ectopic expression of Rac1. (F-H) Quantitative analysis of the alteration in structural  
40 plasticity of dendritic spikes by Rac1. Density in (F), length in (G) and dynamics in (H). The  
41 temporal color codes are red-green-blue in (A) and (E). The numbers in the bar diagrams represent  
42 the sample sizes of each experimental group from three to seven *Drosophila* larvae. For all  
43 quantifications, data are the means  $\pm$  SEM. Unpaired two-sided Student's t-test in (B-D) and (F-H).  
44 \* $p < 0.05$ , \*\* $p < 0.01$ , \*\*\* $p < 0.001$ . Scale bars: 20  $\mu\text{m}$  in (A, left), 10  $\mu\text{m}$  in (A, right) and (E).  
45



46 **Supplementary information, Figure S4**



47

48 Figure S4 The range of emission wavelengths of the four fluorescent proteins labelling organelles.

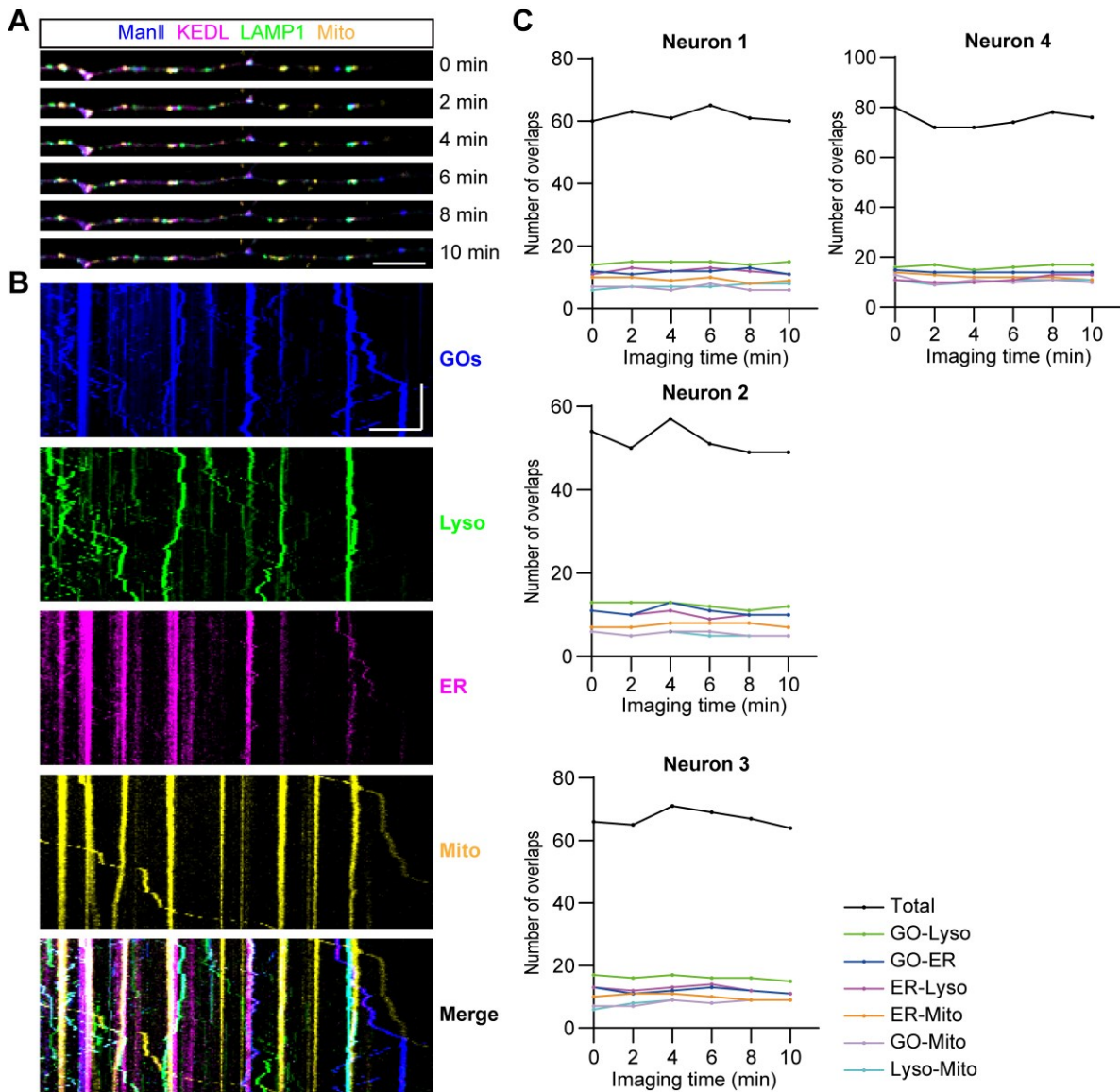
49 Confocal images of singly labelled neurons were recorded at the four wavelength ranges upon the

50 excitation with 405 nm, 488 nm, 543 nm and 633 nm, respectively. Green arrowheads indicate soma

51 and yellow arrows indicate dendrites. Scale bar: 15  $\mu$ m.

52

53 **Supplementary information, Figure S5**



54

55 Figure S5 Dynamic but stable numbers of contacts between dendritic GOs, ER, Lyso and Mito over  
 56 time. (A, B) Representative confocal images of dendrite expressing the four organelle markers at six  
 57 time points (0, 2, 4, 6, 8 and 10 min) (A) and the corresponding kymographs (B) obtained from time-  
 58 lapse imaging show the dynamic contacts between the four organelles. GOs, ER, Lyso and Mito were  
 59 labelled with ManII-mTagBFP2, KDEL-RFP, LAMP1-GFP and Mito-mCardinal, respectively. (C)  
 60 Numbers of the total contacts and contacts between each organelle pair in dendrites of four neurons

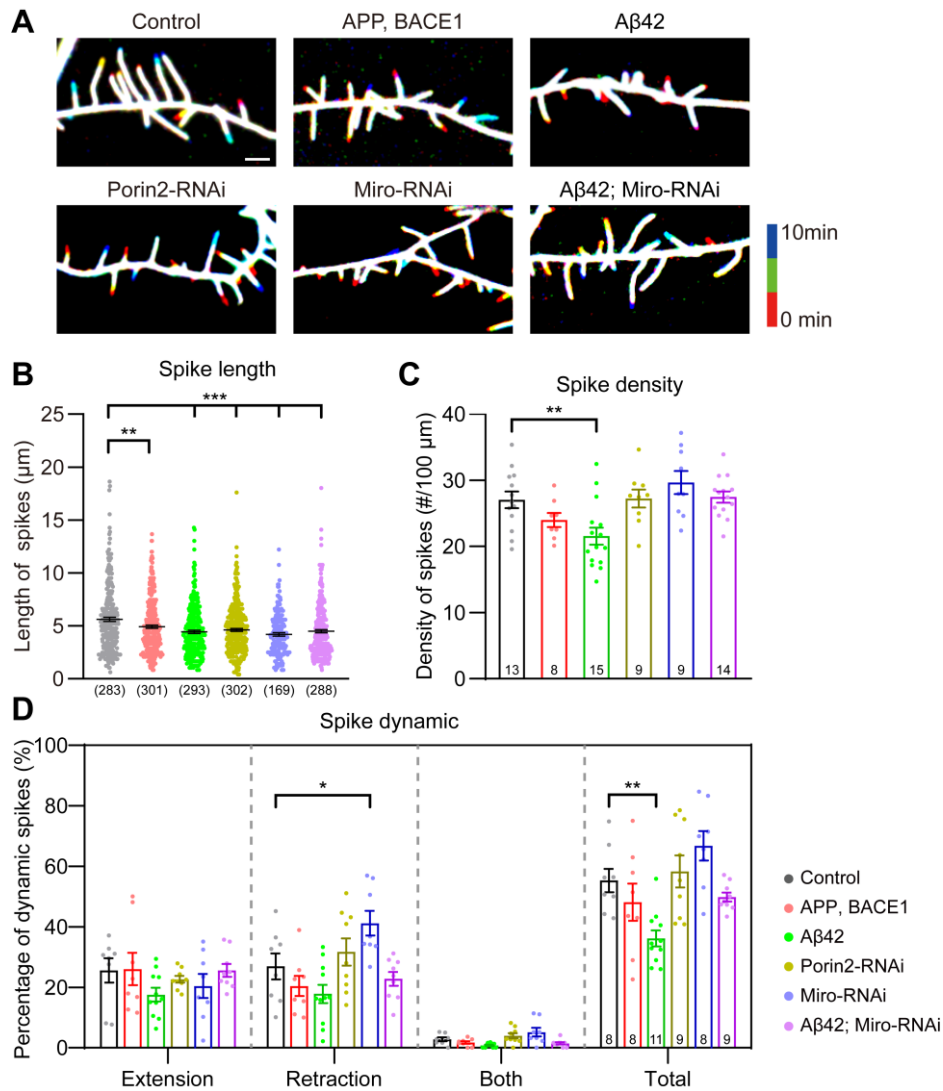
61 over 10 min. Analysis of their coefficients of variation showed that they were all not exceeding 15%,

62 and the average was 7.9%. Horizontal scale bar: 10  $\mu\text{m}$  and vertical bar: 3 min.

63



64 **Supplementary information, Figure S6**



65

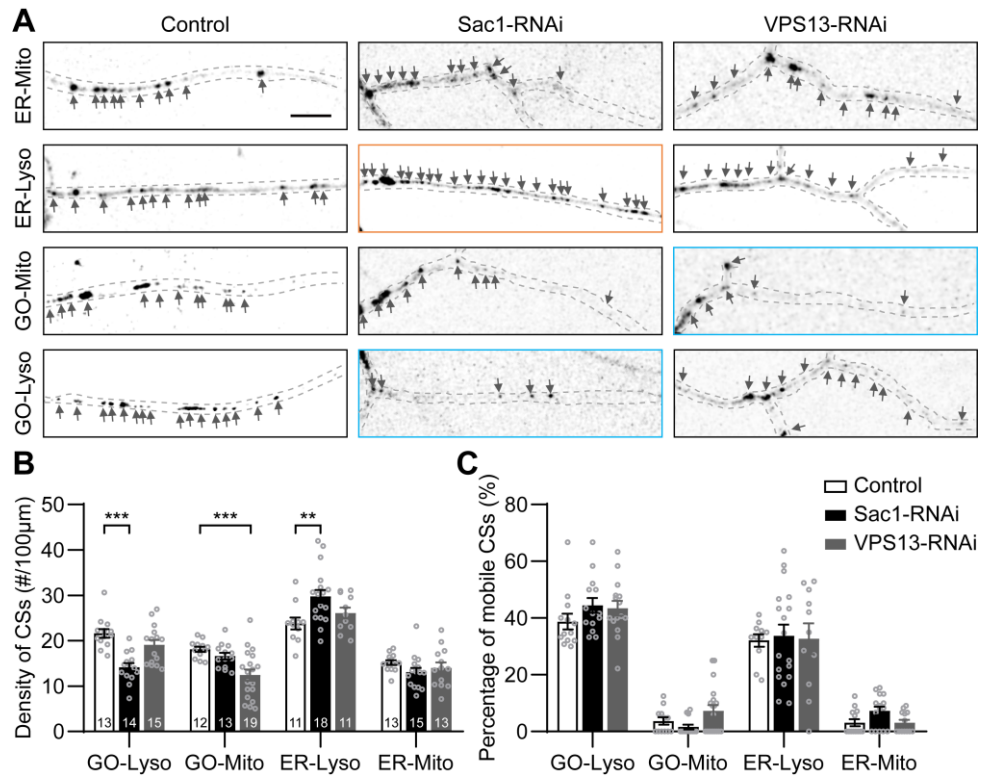
66 Figure S6. The defects and rescue in structural plasticity of dendritic spikes in APP amyloidogenic  
 67 processing. (A) Representative images showing the dynamic dendritic spikes under different  
 68 conditions: normal,  $\beta$ -APP, and A $\beta$ 42 conditions (upper panel); and the manipulation of the CS  
 69 tethers in normal and A $\beta$ 42 neurons (bottom panel). The dendritic spikes were labelled with VSVG-  
 70 GFP, and their dynamics in 10 min were demonstrated by using temporal-code LUT of red-green-  
 71 blue. (B-D) Quantitative analysis of the structural plasticity of dendritic spikes. Length in (B),  
 72 density in (C), and dynamic in (D). The numbers in the bar diagrams represent the sample sizes of  
 73 each experimental group from three to six *Drosophila* larvae. For all quantifications, data are the

74 means  $\pm$  SEM. One-way ANOVA multiple comparisons test with Dunnett correction in (B-D). \*p <

75 0.05, \*\*p < 0.01, \*\*\*p < 0.001. Scar bar: 5  $\mu$ m in (A)

76

77 **Supplementary information, Figure S7**



78

79 Fig. S7 Modulations of the GELM CSs by non-mitochondrial CS tethers. (A) Representative  
 80 confocal images of four types of the GELM CSs in wild-type neurons and neurons with knockdown  
 81 of the CS tethers *Sac1* and *VPS13*. The CSs were labelled by split-GFP probes, and indicated with  
 82 arrows. Dendrites in blue boxes show decreases in CS density and orange ones show the increases.  
 83 (B, C) Quantitative analysis of the densities (B) and motilities (C) of four types of CSs. The numbers  
 84 in the bar diagram represent the sample sizes of each experimental group from four to seven  
 85 *Drosophila* larvae. For all quantifications, data are the means  $\pm$  SEM. One-way ANOVA multiple  
 86 comparisons test with Dunnett correction in (B, C). \*\*p < 0.01, \*\*\*p < 0.001. Scar bar: 10  $\mu$ m in (A)